RESEARCH ARTICLE

WILEY

hsa_circ_0000285 facilitates thyroid cancer progression by regulating miR-127-5p/CDH2

Bowei Zhang[1,2] | Qiaoling Li[3] | Zhe Song[1,2] | Li Ren[1,2] | Yi Gu[1,2] | Chao Feng[1,2] | Jinju Wang[1,2] | Tong Liu[1,2] ![ORCID]

[1]Department of Vascular and Thyroid Surgery, Sichuan Provincial People's Hospital, University of Electronic Science and Technology of China, Chengdu, China

[2]Chinese Academy of Sciences Sichuan Translational Medicine Research Hospital, Chengdu, China

[3]Department of Medical Cosmetology, Chengdu Second People's Hospital, Chengdu, China

Correspondence
Tong Liu, Department of Vascular and Thyroid Surgery, Sichuan Provincial People's Hospital, University of Electronic Science and Technology of China, Chinese Academy of Sciences Sichuan Translational Medicine Research Hospital, No. 32, West Second Section, First Ring Road, Qingyang District, Chengdu 610072, Sichuan, China.
Email: tongliu31@163.com

Abstract

Thyroid cancer (THCA) is a leading endocrine cancer and becomes the fifth most commonly diagnosed malignancy in females. It is confirmed that circular RNAs (circRNAs) perform regulatory potencies in the pathological progress of THCA. Our purpose was to certify the trait of hsa_circ_0000285 (circ_0000285) and investigate its modulatory mechanism in THCA progression. We identified the expression profile of hsa_circ_0000285 in THCA by conducting qRT-PCR assay. Therewith, the potential of hsa_circ_0000285 in THCA development was determined with a set of functional experiments, including CCK-8, wound healing assay, Western blot, and xenograft model. The molecular mechanism underlying hsa_circ_0000285 was investigated with bioinformatic analysis, RIP and dual-luciferase reporter experiments. As opposed to normal samples and cells, hsa_circ_0000285 level was overtly increased in THCA specimens and cells. The downregulation of hsa_circ_0000285 weakened the proliferative and migratory capacity of THCA cells and promoted cell apoptosis. In addition, hsa_circ_0000285 silence suppressed the tumor growth of xenograft model mice in vivo. Notably, we demonstrated that hsa_circ_0000285 might target miR-127-5p/CDH2 axis in THCA. Afterward, our findings manifested that miR-127-5p attenuation blocked the function of hsa_circ_0000285 depletion in THCA cells. In the final step, CDH2 was proven to mediate the repressive potency of miR-127-5p in the malignant behaviors of THCA. Mechanistically, hsa_circ_0000285 induced the development of THCA via functioning as a competing endogenous RNA (ceRNA) of miR-127-5p to enhance CDH2 expression, which provided a new perspective for THCA therapy.

KEYWORDS
CDH2, circRNA, hsa_circ_0000285, miR-127-5p, thyroid cancer

1 | INTRODUCTION

Thyroid cancer (THCA) emanating from thyroid follicular epithelia or par follicular cells remains the most prevailing malignant tumor in the endocrine gland.[1,2] THCA has become a global focus due to its rapidly escalating incidence over recent decades.[3] More importantly, the morbidity of THCA exhibits the fastest growing rate of all cancers.[4] The prevalence of THCA among women is treble male

incidence, and THCA is perceived as the fifth leading malignancy in female population.[5] Worldwide, epidemiological reports indicate that the fatality rate for THCA is about 0.2–0.6 per 100,000 population.[6] The increased incidence is attributable to multiple factors, such as great advances in cross-sectional imaging, premature exposure to ionizing radiation, obesity, endocrine disorders which are caused by the environment and smoking.[7] Despite striking improvements in the diagnosis and management of THCA, its recurrence and overall survival rates remain frustrating.[8] Consequently, more biomolecular studies are necessary to elaborate the pathological process of THCA.

A few years ago, circular RNAs (circRNAs) were established as non-coding RNAs; however, emerging reports have suggested that they may in fact serve as templates for protein translation.[9,10] Most circRNAs are generated from pre-mRNAs by a specific splicing mechanism known as back-splicing involving circularization of the adjacent exons.[11] Compared with their linear subtypes, circRNAs are more stable and show stronger resistance to RNA degradation owing to their special circular structures.[12] The plenty of literature prove that circRNAs can serve as promising molecular indicators for a wide range of human disorders, including cancer.[13] Further, surging evidence testifies the crucial position of circRNA in the oncogenesis of THCA.[14,15] For instance, circRNA WHSC1 contributes to endometrial cancer via targeting miR-646-meidated NPM1.[16] hsa_circ_001783 facilitates breast cancer through acting as a miR-200c-3p sponge.[17] The tumorigenicity of hsa_circ_0000285 has been affirmed in diverse malignancies, such as hepatocellular carcinoma,[18] osteosarcoma,[19] laryngocarcinoma,[20] and even THCA.[21] Nonetheless, the mechanism governing hsa_circ_0000285 in biological processes of THCA have not been fully elucidated.

Herein, the current work is designed to explain the potential molecular mechanism for hsa_circ_0000285 in the occurrence and deterioration of THCA. Mechanically, hsa_circ_0000285 is a promoting factor in the pathology of thyroid cancer via sponging miR-127-5p to target CDH2.

2 | METHODS

2.1 | Clinical specimens

In total, 40 pairs of cancerous samples and non-cancer specimens were supplied by THCA patients undergoing resection at Sichuan Provincial People's Hospital, University of Electronic Science and Technology of China from 2019 to 2020. All patients provided informed consent. No radiotherapy or chemotherapy was carried out prior to thyroidectomy. Tissue samples were instantly treated by liquid nitrogen once resection and reserved at −80°C for future usage. This research passed the approval of the Ethics Committee of Sichuan Provincial People's Hospital, University of Electronic Science and Technology of China.

2.2 | Cell culture and transfection

Human normal thyroid follicular epitheliums Nthy-ori 3-1 and two human THCA cell lines (KTC-1 and TPC-1) were all provided by Chinese Academy of Sciences (Shanghai, China). All cells were cultivated in RPMI-1640 medium (HyClone, USA) added with 10% FBS (Hyclone) in an incubator set at 37°C with suitable humidity under 5% CO_2.

To silence hsa_circ_0000285 and CDH2, small-interfering RNA (siRNA) oligonucleotides targeting hsa_circ_0000285 and CDH2 were constructed by GenePharma (Shanghai, China) with scramble siRNA (si-NC) oligonucleotides as negative control. The oligonucleotides for overexpression or inhibition of miR-127-5p were obtained from Geneseed (Guangzhou, China). Oligonucleotides were transfected into THCA cells by virtue of Lipofectamine 2000 (Invitrogen, USA) as demanded by the product descriptions.

2.3 | Quantitative real-time polymerase reaction

Trizol reagent bought from Invitrogen was exploited for total RNA isolation. Afterward, RNA quantification was performed by the ND-2000 spectrophotometer (Life Technologies, USA). The Prime Script RT Kit (Toyobo, Japan) was adopted for cDNA synthesis. A specific stem-loop primer was used as the reverse transcription primer to synthesize cDNA for miR-127-5p amplification (RT-miR-127-5p: 5′-CTCAACTGGTGTCGTGGAGTCGGCAATTCAGTTGAGAATCAGAG -3′). In brief, 10 μL of the reaction mixture containing 1× PrimeScrip Buffer, 1 μL PrimeScrip RT Enzyme Mix I, 100 ng RNA and special stem-loop RT primers were incubated for 30 min at 16°C, followed by a pulsed reverse transcription reaction with the following conditions: 60 cycles at 30°C for 30 s, 42°C for 30 s and 50°C for 1 s; the reaction was then stopped by the inactivation of the PrimeScrip RT Enzyme at 85°C for 5 s. The PCR detection was implemented in real-time PCR system (Applied Biosystems, USA) employing SYBR Green

TABLE 1 Primers used in the present work

Targets	Primers sequences (5′ to 3′)
circ_0000285	Forward: 5′-GCTCAGTTTGGTTGTGGTGA
	Reverse: TCACATGAATTTAGGTGGGACTT
miR–127-5p	Forward: 5′-ACACTCCAGCTGGGCTGAAGCTCA GAGGGCTC–3′
	Reverse: 5′-CTCAACTGGTGTCGTGGA–3′
SDC4	Forward: 5′-TCCGAGAAACTGAGGTCATCGAC
	Reverse: GGTACACCAGCAGCAGCACGAG
CDH2	Forward: 5′-AGCCAACCTTAACTGAGGAGT
	Reverse: GGCAAGTTGATTGGAGGGATG
U6	Forward: 5′-AT TGGAACGATACAGAGAAGATT 3′
	Reverse: 5′-GGAACGCT TCACGAATTTG 3
GAPDH	Forward: 5′-AACGGATTTGGTCGTATTGG
	Reverse: TTGATTTTGGAGGGATCTCG

Master Mix (Roche, USA) on the basis of the product protocols, 1.6 μL cDNA product along with 2 μL PCR primers, 10 μL SYBR Green Master, and 6.4 μL DEPC water. The PCR conditions included denaturing at 95°C for 10 min, followed by 40 cycles of 95°C for 15 s and 60°C for 1 min. The abundance of mRNA or miRNA was normalized to the housekeeping gene GAPDH or U6. Gene expression was quantified with the $2^{-\Delta\Delta Ct}$ method. The sequences of primers are listed in Table 1.

2.4 | Nuclear-cytoplasmic fractionation

In short, extraction of nuclear and cytoplasmic RNA was conducted by utilization of the PARIS kit (Invitrogen) according to the recommendations supplied by the manufacturer. hsa_circ_0000285 expression in subcellular fractions was determined with Quantitative real-time polymerase reaction (qRT-PCR) analysis. GAPDH was cytoplasmic reference, and U6 was nuclear reference.

2.5 | RNase R treatment assay

Following RNA isolation, total RNA was subjected to RNase R treatment (3 U/μg, Thermo Fisher Scientific, USA) at 37°C for 30 min,

purified with the RNeasy MinElute Cleaning Kit (QIAGEN, Germany) and finally detected by qRT-PCR assay.

2.6 | Cell Counting Kit-8

THCA cell proliferation was tested with Cell Counting Kit-8 (CCK-8) (Sigma, USA) pursuant to the directions of the vender. KTC-1 and TPC-1 cells were seeded to 96-well plates at 3000 cells/well and cultivated in the standard condition (37°C, 5% CO_2). At indicated times (24, 48, 72, and 96 h), cells were incubated with CCK-8 solution for 2 h and subsequently cell viability was examined via measuring OD value at 450 nm utilizing a microplate reader (Molecular Devices, USA).

2.7 | Wound healing assay

Transfected THCA cells were plated to 6-well plates and cultivated under 5% CO_2 at 37°C. Until 80%–90% confluence, the scratch was produced by a 100 μl sterile pipette tip. Following the removal of the debris, cells were incubated at 37°C and imaged with a microscope (Olympus, Japan). Wound width was recorded at 0 and 24 h after cell layer injury.
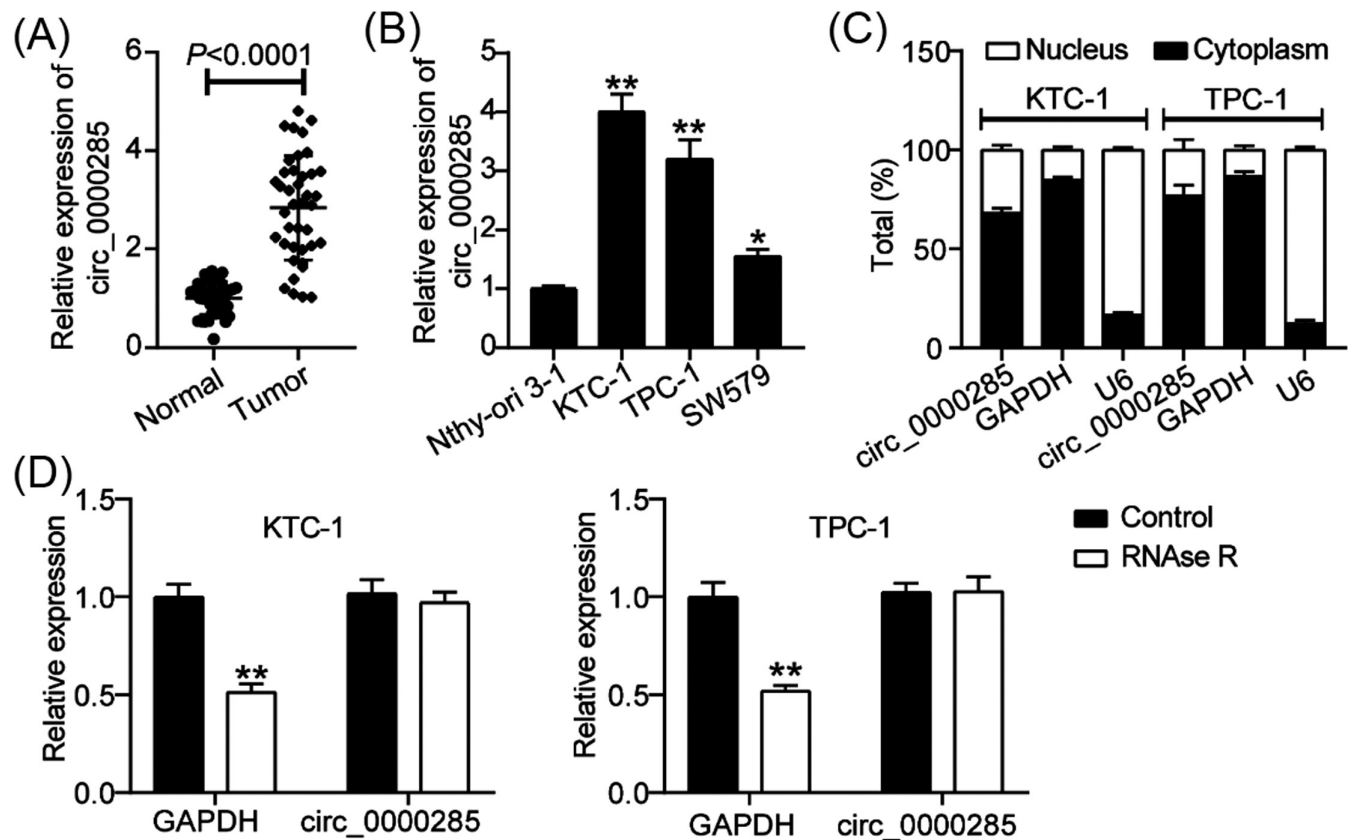

FIGURE 1 hsa_circ_0000285 level was remarkably elevated in THCA. (A-B) The qRT-PCR measurement of hsa_circ_0000285 expression in THCA clinical specimens and cell lines. (C) The subcellular analysis of circ_0000285 in THCA cells. (D) The traits of hsa_circ_0000285 verified by RNase R treatment assay. vs. matched control group, $^*p < 0.05$, $^{**}p < 0.01$
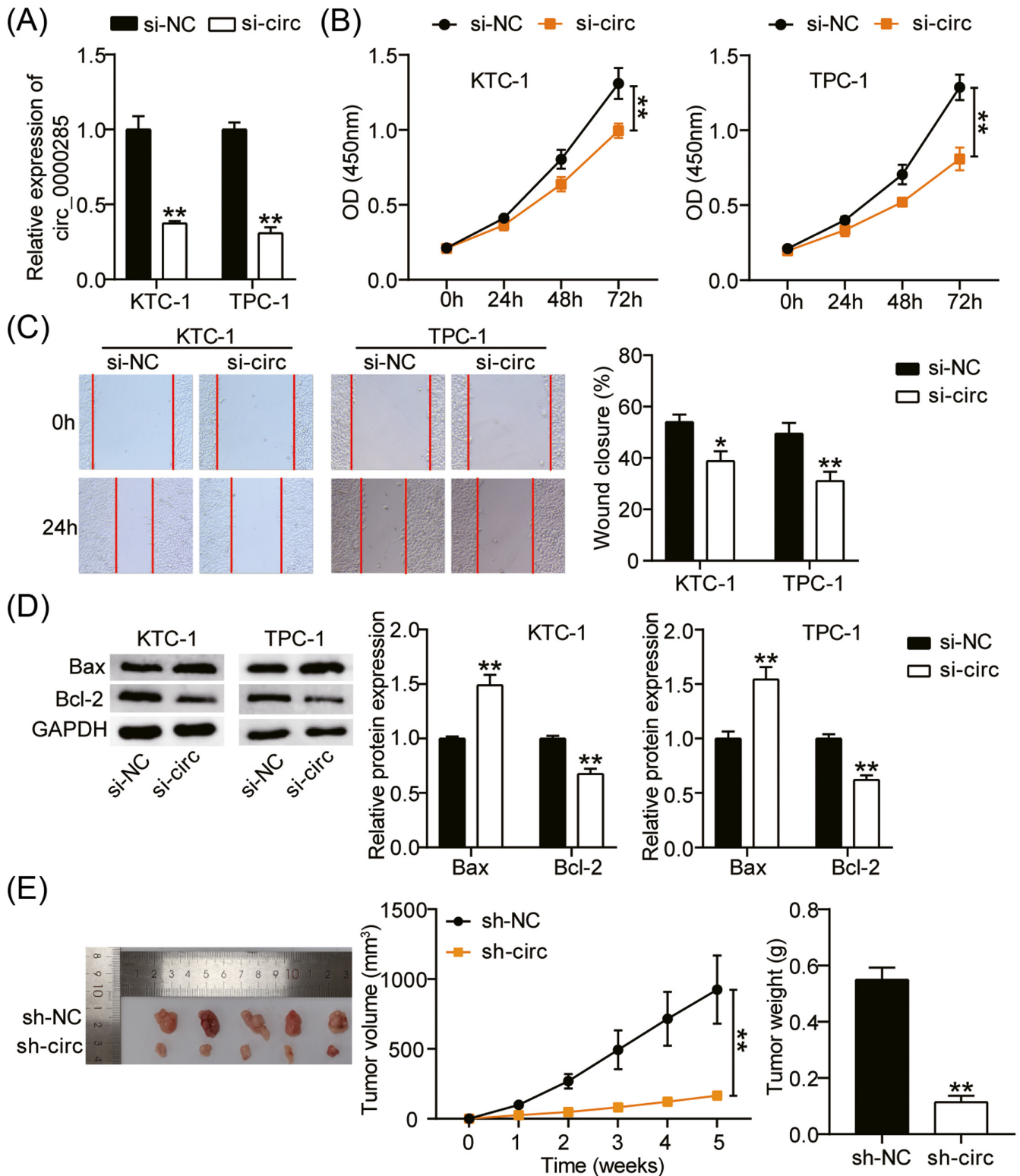
FIGURE 2 Suppressing hsa_circ_0000285 weakened the malignancy of THCA. (A) hsa_circ_0000285 level in transfected THCA cells. (B) THCA cell viability examined by CCK-8 detection. (C) Wound healing experiment was conducted for cell migration assessment. (D) The protein expression of Bax and Bcl-2. (E) The size and weight of neoplasms in xenograft tumor models. vs. si-NC, $^*p < 0.05$, $^{**}p < 0.01$

2.8 | RNA immunoprecipitation

With the aid of the EZMagna RNA immunoprecipitation (RIP) Kit (Millipore, USA), RIP assay was carried out following the product manuals. After transfection, THCA cells were dissolved in RIP lysis buffer. Next, the lysates were immunoprecipitated by using magnetic beads and Ago2 antibody (Millipore) or negative control IgG antibody (Millipore). Following incubating all the night at 4°C,
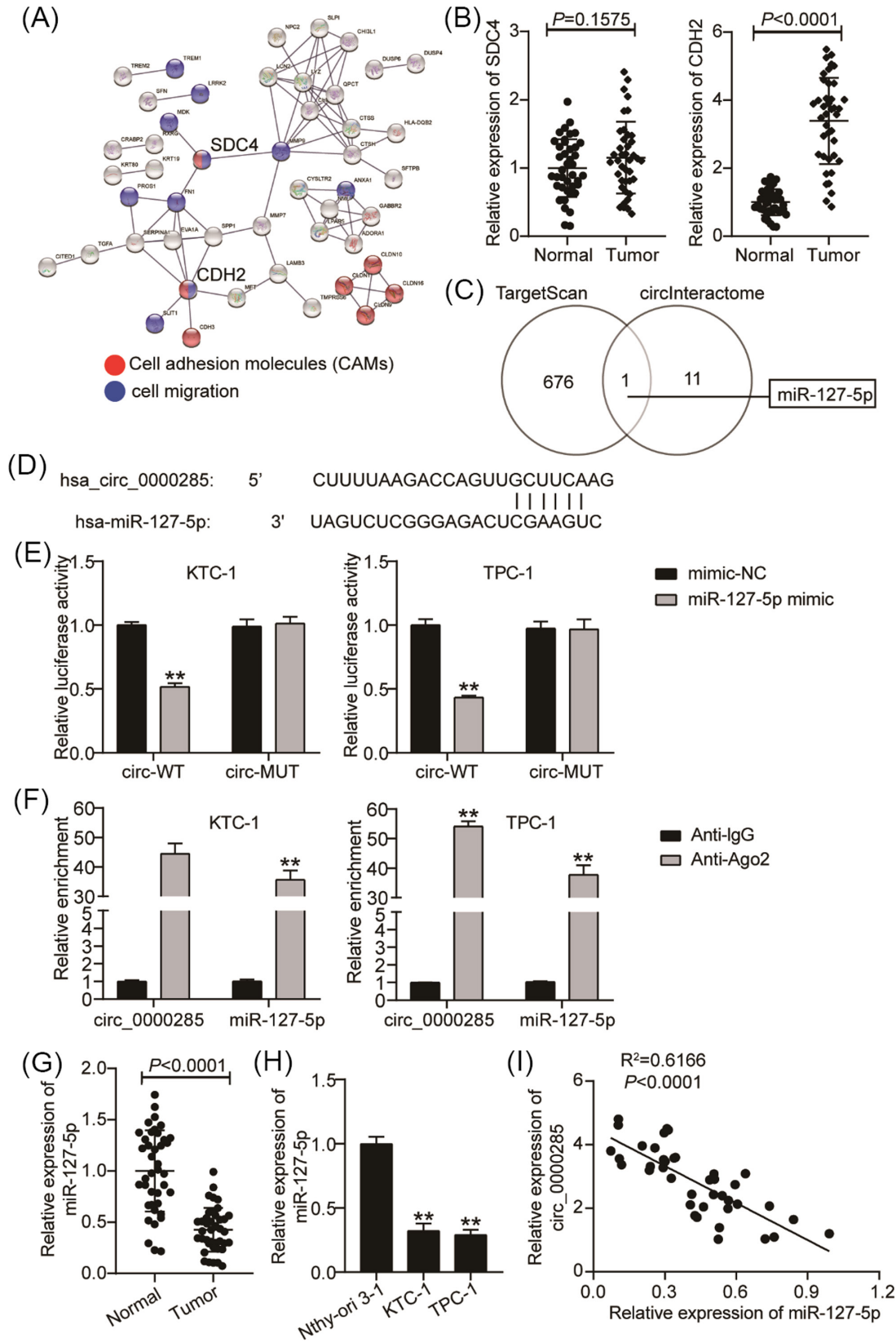
FIGURE 3 miR-127-5p/CDH2 axis might be targeted by hsa_circ_0000285. (A) SDC4 and CDH2 were related to cell adhesion and cell migration according to the STRING analysis. (B) SDC4 and CDH2 levels in THCA and adjacent normal tissues. (C) miR-127-5p was overlapped from TargetScan and circInteractome. (D) The conjectured binding sites of hsa_circ_0000285 for miR-127-5p based on circInteractome database. (E-F) The interplay of hsa_circ_0000285 with miR-127-5p was identified utilizing dual-luciferase reporter test and RIP. vs. mimic-NC or Anti-IgG group, **$p < 0.01$. (G-H) miR-127-5p expression in THCA at tissue (G) and cell level (H). vs. Normal or Nthy-ori 3-1 cells, **$p < 0.01$. (I) The negative association of hsa_circ_0000285 with miR-127-5p in THCA tissues
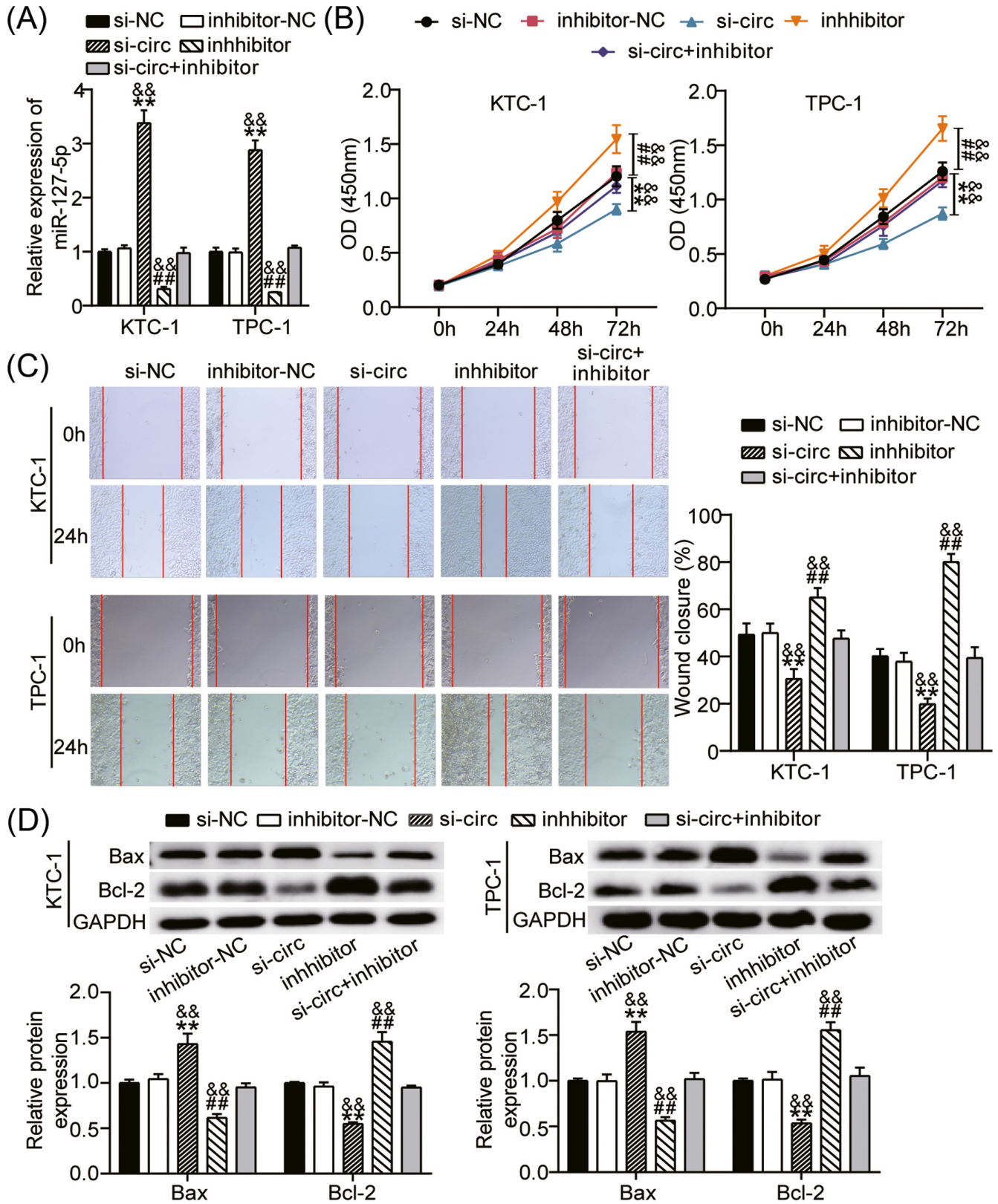
FIGURE 4 miR-127-5p mediated the potency of hsa_circ_0000285 in THCA cell growth, migration, and apoptosis. (A) miR-127-5p expression in transfected THCA cells. (B) CCK-8 assay. (C) Wound healing assay. (D) The potential of miR-127-5p in cell apoptosis was assessed with Western blot. vs. si-NC, **$p < 0.01$. vs. inhibitor-NC, ##$p < 0.01$. vs. si-circ+inhibitor, $^{\$\$}p < 0.01$

FIGURE 5 CDH2 was targeted by miR-127-5p. (A) TargetScan predicted potential miR-127-5p binding sites in CDH2. (B) Dual-luciferase reporter experiment certified that miR-127-5p combined with CDH2. vs. mimic-NC, **p < 0.01. (C) CDH2 expression in normal cells and THCA cells. vs. Nthy-ori 3-1 cells, **p < 0.01. (D) Pearson correlation analysis between miR-127-5p and CDH2 in THCA tissues
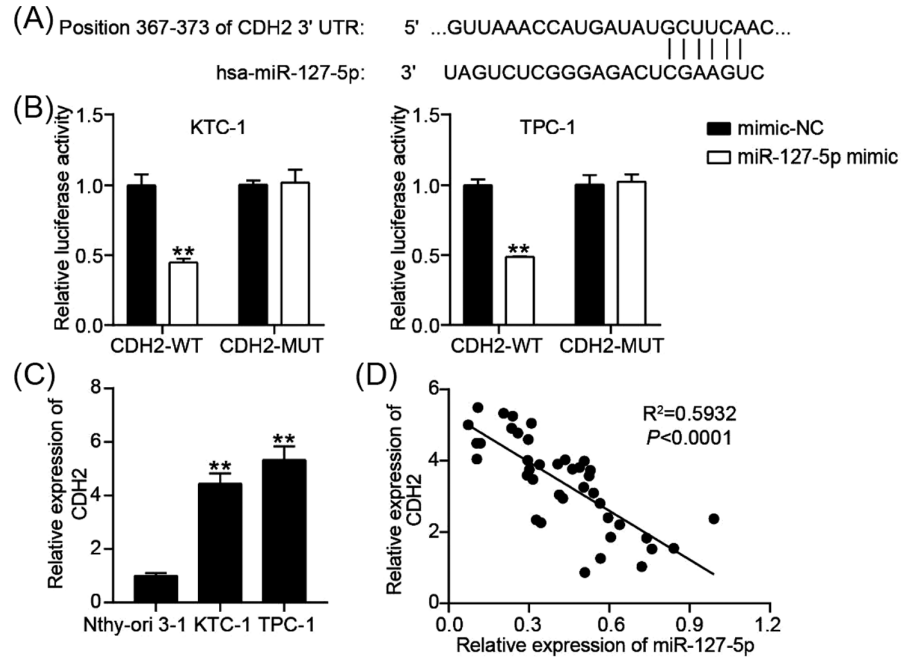
RNA-protein mixtures were eluted from magnetic beads, and thereafter Proteinase K treatment was used for RNA isolation. The abundance of hsa_circ_0000285 and miR-127-5p was analyzed with qRT-PCR assay.

2.9 | Animal assay

To establish xenograft tumor models, 6-week-old BALB/c nude mice supplied by Vital River Laboratory Animal Company (Shanghai, China) were applied and raised at 23 ± 3°C under a relative humidity of 55% ± 15% specific pathogen-free (SPF) condition with 12 h:12 h light:dark cycle. 34 mice were distributed into sh-NC group and sh-hsa_circ_0000285 group. Following stable transfection with shRNA for hsa_circ_0000285 or negative control sh-NC vectors, KTC-1 cells were inoculated into nude mice. Tumor growth was plotted via measuring the size of the xenograft tumor. Five weeks later, mice were euthanatized, and neoplasms were weighed. All experimental procedures complied with the guiding principles set by the Animal Care and Use Committee of Sichuan Provincial People's Hospital, University of Electronic Science and Technology of China.

2.10 | Western blot

THCA cells were dissolved by RIPA lysis buffer (Thermo Fisher Scientific) containing protease inhibitor (Beyotime, Shanghai, China). BCA kit (Beyotime) was employed for the examination of total protein concentration. Protein aliquots were segregated on 10%

SDS-PAGE gel, electrophoretically transferred to the PVDF membranes, and sealed in 5% skim milk for about 2 h at 37°C. Following incubation with specific antibodies at 4°C overnight, membranes were probed by secondary antibodies at 37°C for 1–2 h. Lastly, the ECL kit (Beyotime) was used to detect protein expression. Listed primary antibodies were utilized: Bax (Abcam, USA), Bcl-2 (Abcam), CDH2 (Cell Signaling Technology, USA), and GAPDH (Abcam). GAPDH was exploited as the loading control.

2.11 | Dual-luciferase reporter assay

hsa_circ_0000285 and CDH2 sequences containing or without conjectured miR-127-5p sites were ligated into pmirGLO plasmids (Promega, USA) to obtain hsa_circ_0000285-wt, hsa_circ_0000285-mut, CDH2-wt, and CDH2-mut, respectively. The corresponding vectors were co-transfected into THCA cells with miR-127-5p mimic or miR-NC. Through employment of Dual-Luciferase Reporter Assay Kit (Promega), the luciferase activity was detected at 24 h post transfection.

2.12 | Statistical analysis

Data processing was conducted by GraphPad Prism 6.0 (GraphPad, USA). All results were recorded by means ± SD. Each experiment was carried out three times independently. Comparison among groups was conducted with Student's t test or one-way ANOVA. The targeting relationship was determined by Pearson correlation. p < 0.05 manifested statistical significance.
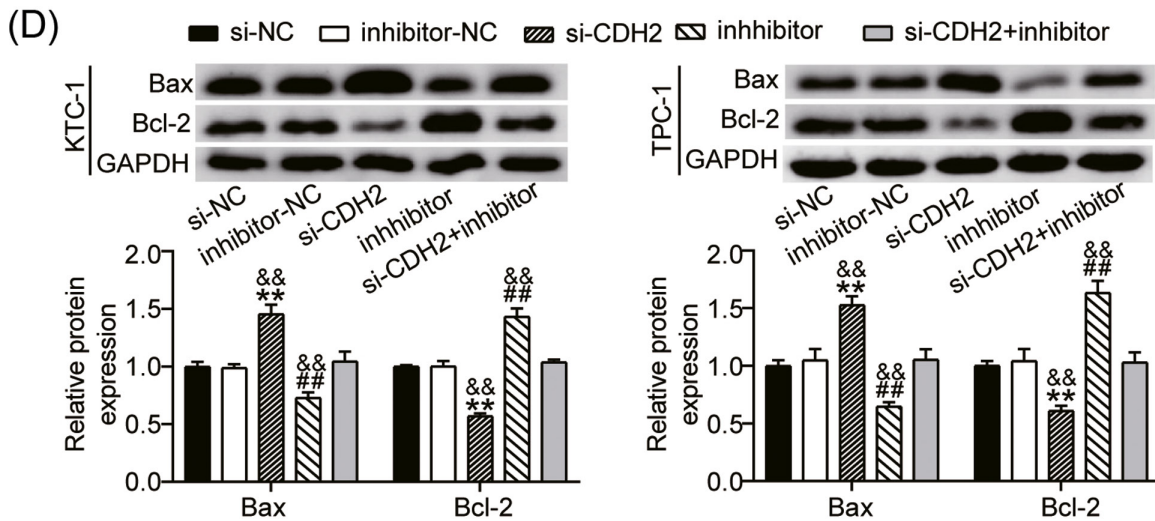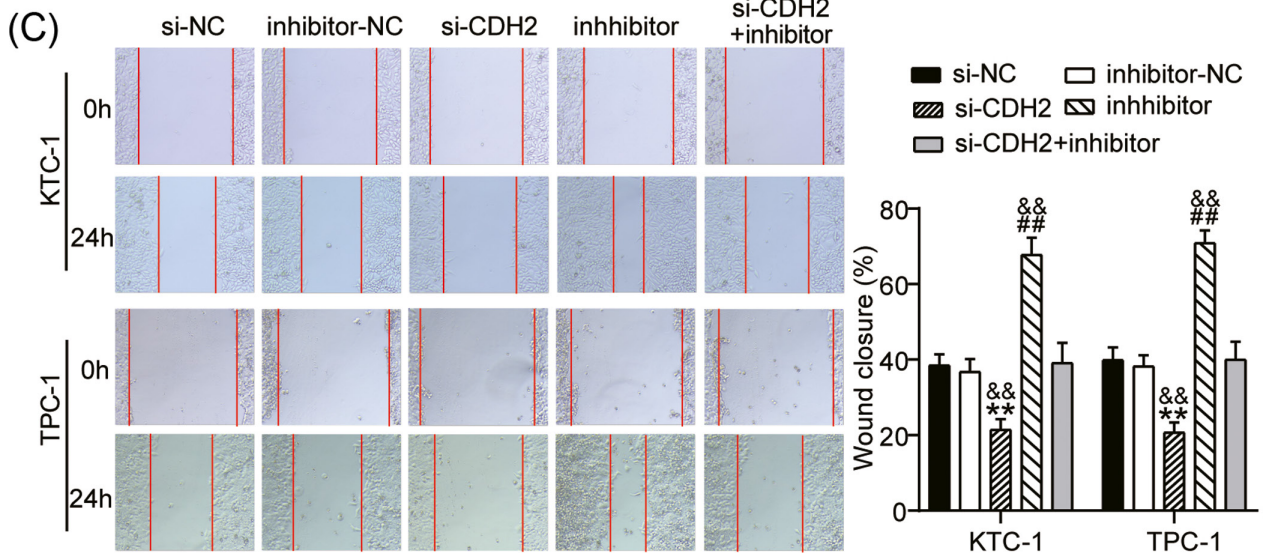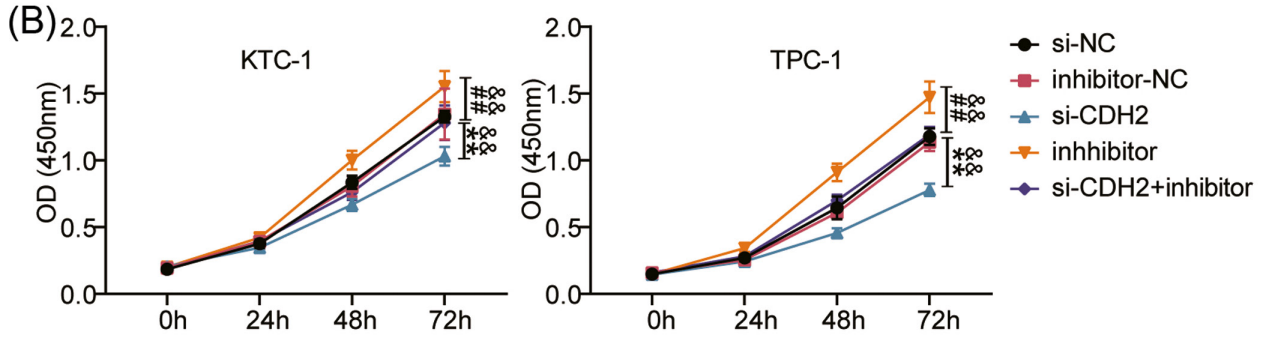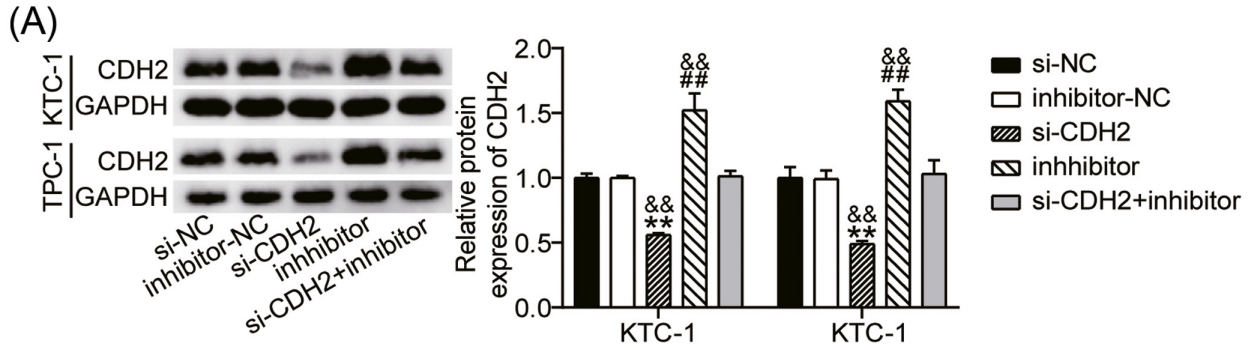
(A)

(B)

(C)

(D)

FIGURE 6 miR-127-5p alleviated the aggressive traits of THCA cells through CDH2. (A) qRT-PCR analysis of CDH2 level in transfected THCA cells. (B) CCK-8 assay was employed for estimation of cell proliferation. (C) Cell migratory capacity was detected using wound healing experiment. (D) Western blot results of Bax and Bcl-2 expression. vs. si-NC, $^{**}p < 0.01$. vs. inhibitor-NC, $^{##}p < 0.01$. vs. si-CDH2+inhibitor, $^{\$\$}p < 0.01$

3 | RESULTS

3.1 | hsa_circ_0000285 level was remarkably elevated in THCA

Firstly, we aimed to affirm the expression pattern of hsa_circ_0000285 in THCA. qRT-PCR assay suggested that hsa_circ_0000285 was abundantly expressed in THCA specimens compared with normal tissue sample (Figure 1A). In contrast with Nthy-ori 3-1 cells, KTC-1 and TPC-1 cells exhibited higher hsa_circ_0000285 expression level (Figure 1B). Besides, our observations disclosed that hsa_circ_0000285 was principally located in cytoplasmic regions of KTC-1 and TPC-1 cells, implying that hsa_circ_0000285 might involve in THCA progression via a competing endogenous RNA (ceRNA) network (Figure 1C). Then, the circRNA feature of hsa_circ_0000285 was measured by RNase R treatment. As shown in Figure 1D, hsa_circ_0000285 showed more stability for RNase R than its linear RNA (Figure 1D).

3.2 | Suppressing hsa_circ_0000285 weakened the malignancy of THCA

Subsequently, loss-of-function assays were performed to identify the role for hsa_circ_0000285 in cell biology of THCA. Through transfection with si-circ_0000285 plasmids, hsa_circ_0000285 was knocked down in THCA cells (Figure 2A). Afterward, we observed that downregulation of hsa_circ_0000285 caused the obvious decrease in THCA cell viability (Figure 2B). Wound healing experiment manifested that the migratory capacity of THCA cells was impaired when hsa_circ_0000285 was silenced (Figure 2C). Likewise, Western blot analysis showed that depletion of hsa_circ_0000285 augmented Bax level, whereas lessened the expression of Bcl-2 (Figure 2D). In concert with the foregoing, in vivo assay validated that hsa_circ_0000285 knockdown significantly diminished the size and weight of tumor tissue in nude mice (Figure 2E). To sum up, hsa_circ_0000285 was an oncogene in THCA.

3.3 | circ_0000285 might target miR-127-5p/CDH2 axis in THCA

According to GEPIA data, 172 upregulated genes in THCA samples were screened with adj.$p < 0.05$ and logFC ≥ 2 (Supporting Information Table S1). Uploading 172 upregulated genes to STRING, it was found that SDC4 and CDH2 were related to cell adhesion and cell migration (Figure 3A). After preforming qRT-PCR, CDH2 was significantly upregulated in THCA compared with SDC4 (Figure 3B); hence, CDH2 was confirmed as our interested gene. Next, TargetScan and circInteractome found out the miRNAs possessing affinity with CDH2 or hsa_circ_0000285. Notably, miR-127-5p was a common miRNA (Figure 3C). The bioinformatics analysis suggested that hsa_circ_0000285 might affect miR-127-5p/CDH2 axis. The potential miR-127-5p binding sites in hsa_circ_0000285 acquired from circInteractome were displayed (Figure 3D). Accordingly, we conducted luciferase reporter gene assay to confirm their interaction. Our findings manifested that luciferase activity of hsa_circ_0000285-wt was descended in response to miR-127-5p mimic, while that of hsa_circ_0000285-mut remained unchanged (Figure 3E). RIP experiment further demonstrated that hsa_circ_0000285 bound to miR-127-5p (Figure 3F). Additionally, it was disclosed that miR-127-5p was weakly expressed in THCA at tissue and cell levels (Figure 3G-H). Correlation analysis illustrated that hsa_circ_0000285 was negatively associated with miR-127-5p (Figure 3I). Collectively, we concluded that hsa_circ_0000285 might regulate CDH2 in a miR-127-5p-dependent manner.

3.4 | miR-127-5p mediated the potency of hsa_circ_0000285 in THCA cell growth, migration, and apoptosis

To verify the influences of hsa_circ_0000285/miR-127-5p axis, rescue assays were carried out. qRT-PCR detection data revealed that silencing hsa_circ_0000285 enhanced the expression of miR-127-5p and the recovery of miR-127-5p level occurred when miR-127-5p was inhibited (Figure 4A). The CCK-8 assay unraveled that miR-127-5p repression reversed cell viability induced by hsa_circ_0000285 depletion (Figure 4B). Similarly, the inhibition of cell migration caused by hsa_circ_0000285 downregulation was abated by miR-127-5p inhibitor (Figure 4C). Consistently, the increased Bax expression and reduced level of Bcl-2 were restored owing to suppression of miR-127-5p (Figure 4D). These findings provided strong evidence that hsa_circ_0000285 modulated THCA cell behaviors through sponging miR-127-5p.

3.5 | CDH2 worked as a target gene of miR-127-5p

By utilization of TargetScan, miR-127-5p was found to possess the potential binding sites for CHD2 (Figure 5A). Therewith, we intended to determine the combining capability of CHD2 with miR-127-5p. Our findings expounded that only luciferase activity of CHD2-wt was prominently lowered due to treatment with miR-127-5p mimic, suggesting the interplay of CHD2 with miR-127-5p (Figure 5B).

The expression of CHD2 was higher in KTC-1 and TPC-1 cells than normal thyroid follicular epitheliums (Figure 5C). Moreover, it was proven that CHD2 expression was inversely associated with miR-127-5p level in the expression cohort of clinical tissues (Figure 5D). In other words, CDH2 was a target effector for miR-127-5p.

3.6 | miR-127-5p alleviated the aggressive traits of THCA cells through CDH2

Finally, we aimed to certify miR-127-5p-mediated molecular pathway in the development of THCA. Results of Western blot assay indicated that CDH2 level was increased owing to inhibition of miR-127-5p and then recovered via knockdown of CDH2 in THCA cells (Figure 6A). Further, miR-127-5p inhibitor promoted THCA cell proliferation, while silencing of CDH2 exerted the opposite function and abrogated the influences of miR-127-5p downregulation on THCA cell viability (Figure 6B). Our results illustrated that enhanced cell migration triggered by the suppression of miR-127-5p was abolished by CDH2 downregulation (Figure 6C). Uniformly, miR-127-5p inhibitor led to reduced Bax level and the enhanced expression of Bcl-2, and depletion of CDH2 counteracted the regulatory role of miR-127-5p inhibitor in Bax and Bcl-2 expression (Figure 6D). Based on the mentioned findings, CDH2 was responsible for the impacts of miR-127-5p on the aggressive behaviors of THCA cells.

4 | DISCUSSION

Currently, the complex etiology of THCA is still indistinct. Growing researches have demonstrated that circRNA performs a significant function in the initiation and evolution of human cancer.[22,23] We justified that hsa_circ_0000285 was markedly enhanced in THCA samples and cells. Knockdown of hsa_circ_0000285 retarded THCA cell proliferation, migration, and apoptosis escape. Moreover, hsa_circ_0000285 silence inhibited THCA growth in vivo. Further investigations illuminated that hsa_circ_0000285 worked as a regulator in cell function of THCA by absorbing miR-127-5p. By STRING analysis and qRT-PCR detection, CDH2 was uncovered to be the most significantly upregulated in clinical tumor tissues from THCA patients compared with normal samples among genes associated with cell migration. Notably, our findings indicated that CDH2, a target of miR-127-5p, was accountable to miR-127-5p-mediated THCA cell phenotypes.

It is reported that aberrant expression patterns of circRNAs are commonly observed in carcinoma tissue samples.[24-27] An abundant of studies verify that circRNA is of immense importance in the pathogenesis of THCA. In recent years, the involvement of hsa_circ_0000285 has been investigated in numerous cancers. Increasing findings illustrate that hsa_circ_0000285 executes crucial regulatory properties in tumor progression. For example, the suppression of hsa_circRNA_0000285 impedes

tumorigenesis and autophagy in cervical carcinoma through miR197-3p/ELK1 pathway.[28] hsa_circ_0000285 represents a novel biomarker in bladder cancer on account of its potential in modulating cisplatin resistance.[29] More than that, Yang D et al. attested that hsa_circ_0000285 induced THCA cell metastasis in a miR-599-mediated manner.[30] Based on the previous study, this current research purposed to confirm the carcinogenic function of hsa_circ_0000285 and explore the latent mechanism of hsa_circ_0000285 in cell biology of THCA. As anticipated, we certified the high expression of hsa_circ_0000285 in THCA. Our data firstly unraveled that hsa_circ_0000285 performed a simulative role in cell growth both in vitro and in vivo. Besides, the promoting potency of hsa_circ_0000285 in cell migration was validated by transwell assay.

It is widely acknowledged that circRNAs can serve as ceRNAs to control gene expression by sponging targeted miRNAs to affect their activity and then modulate miRNA-mediated downstream targets.[31-34] Our experimental data suggested the main location of hsa_circ_0000285 in THCA cytoplasm, supporting the conjecture that hsa_circ_0000285 might participate in THCA development via a ceRNA mechanism. A large number of reports expound that CDH2 presents carcinogenic impacts on the malignant behaviors of multiple cancers.[35-38] More importantly, recent study reveals that CDH2 is upregulated in THCA tissues and CDH2 possesses the potential to be a prognostic biomarker.[39] In this study, SDC4 and CDH2 were found to show strong association with cell adhesion and migration among upregulated genes in THCA by virtue of STRING analysis. Additionally, the level of CDH2 was much higher than that of SDC4 in THCA. As a result, CDH2 was chosen for in-depth study. Subsequently, bioinformatics analysis disclosed that miR-127-5p was the candidate miRNA containing the predicted binding sites for hsa_circ_0000285 and CDH2. Although multitudinous documents elaborate that miR-127-5p was a suppressive factor in various types of human cancers, such as hepatocellular carcinoma,[40] gastric cancer,[41] and cervical cancer,[42] its influences on THCA and action mode remain to be identified. The present research manifested that miR-127-5p was negatively modulated by hsa_circ_0000285 and the enhanced function of miR-127-5p inhibitor in aggressive behaviors of THCA cells neutralized the role of hsa_circ_0000285 silence. Moreover, CDH2 was confirmed to act as a direct effector of miR-127-5p and responsible for the impacts of miR-127-5p on THCA.

Even though it was the first study to prove the pathway constituted by hsa_circ_0000285, miR-127-5p and CDH2 promote tumor progression of THCA, some limitations still existed in this work. Considering the well-known association between CDH2 and epithelial-mesenchymal transition (EMT), the role of the signaling axis in EMT should be clarified. Meanwhile, the number of clinical samples was insufficient. To further verify and enrich our findings, we will expand the sample size and add more experiments in the future.

By and large, we illustrated that hsa_circ_0000285 exerted oncogenic functions in THCA via absorbing miR-127-5p to regulate

CDH2 expression, which contributed to comprehensively understanding the pathogenesis of THCA and offered a promising therapeutic strategy for THCA patients.

CONFLICT OF INTEREST

Each author declares no conflict of interest.

AUTHORS' CONTRIBUTIONS

BWZ and QLL were responsible for experiments and data analysis. BWZ and ZS designed the study. LR and YG conducted data acquisition. CF, JJW, and TL analyzed and interpreted the data. All authors reviewed and approved the draft.

CONSENT TO PARTICIPATE

All patients were signed written informed consent.

CONSENT FOR PUBLICATION

Consent for publication was obtained from the participants.

CODE AVAILABILITY

Not available.

DATA AVAILABILITY STATEMENT

The datasets used and/or analyzed during the current study are available from the corresponding author on reasonable request.

ORCID

Tong Liu https://orcid.org/0000-0003-1522-3445

REFERENCES

1. Kitahara CM, Sosa JA. The changing incidence of thyroid cancer. *Nat Rev Endocrinol.* 2016;12(11):646-653.
2. Carling T, Udelsman R. Thyroid cancer. *Annu Rev Med.* 2014;65:125-137.
3. Javed Z, Ahmed Shah F, Rajabi S, et al. LncRNAs as potential therapeutic targets in thyroid cancer. *Asian Pac J Cancer Prev.* 2020;21(2):281-287.
4. Park JY, et al. Role of BRAF and RAS mutations in extrathyroidal extension in papillary thyroid cancer. *Cancer Genomics Proteomics.* 2016;13(2):171-181.
5. Siegel RL, Miller KD, Jemal A. Cancer statistics, 2017. *CA Cancer J Clin.* 2017;67(1):7-30.
6. La Vecchia C, Malvezzi M, Bosetti C, et al. Thyroid cancer mortality and incidence: a global overview. *Int J Cancer.* 2015;136(9):2187-2195.
7. Fiore M, Oliveri Conti G, Caltabiano R, et al. Role of Emerging Environmental Risk Factors in Thyroid Cancer: A Brief Review. *Int J Environ Res Public Health.* 2019;16(7):1185.
8. Luan S, Fu P, Wang X, et al. Circular RNA circ-NCOR2 accelerates papillary thyroid cancer progression by sponging miR-516a-5p to upregulate metastasis-associated protein 2 expression. *J Int Med Res.* 2020;48(9):300060520934659.
9. Schneider T, Bindereif A. Circular RNAs: coding or noncoding? *Cell Res.* 2017;27(6):724-725.
10. Lu Y, Li Z, Lin C, et al. Translation role of circRNAs in cancers. *J Clin Lab Anal.* 2021;35(7):e23866.
11. Chen LL, Yang L. Regulation of circRNA biogenesis. *RNA Biol.* 2015;12(4):381-388.
12. Ebbesen KK, Hansen TB, Kjems J. Insights into circular RNA biology. *RNA Biol.* 2017;14(8):1035-1045.
13. Li X, Yang L, Chen LL. The biogenesis, functions, and challenges of circular RNAs. *Mol Cell.* 2018;71(3):428-442.
14. Guo D, Li F, Zhao X, et al. Circular RNA expression and association with the clinicopathological characteristics in papillary thyroid carcinoma. *Oncol Rep.* 2020;44(2):519-532.
15. Xia F, Zhang Z, Li X. Emerging roles of circular RNAs in thyroid cancer. *Front Cell Dev Biol.* 2021;9:636838.
16. Liu Y, Chen S, Zong Z-H, et al. CircRNA WHSC1 targets the miR-646/NPM1 pathway to promote the development of endometrial cancer. *J Cell Mol Med.* 2020;24(12):6898-6907.
17. Liu Z, Zhou Y, Liang G, et al. Circular RNA hsa_circ_001783 regulates breast cancer progression via sponging miR-200c-3p. *Cell Death Dis.* 2019;10(2):55.
18. Zhang XJ, et al. The role of hsa_circ_0000285 in metastasis of hepatocellular carcinoma. *Eur Rev Med Pharmacol Sci.* 2020;24(13):7204.
19. Long Z, et al. Circ_0000285 regulates proliferation, migration, invasion and apoptosis of osteosarcoma by miR-409-3p/IGFBP3 axis. *Cancer Cell Int.* 2020;20:481.
20. Qin JB, et al. Circular RNA hsa_circ_0000285 acts as an oncogene in laryngocarcinoma by inducing Wnt/β-catenin signaling pathway. *Eur Rev Med Pharmacol Sci.* 2020;24(19):9773.
21. Yang D, et al. The interaction between circular RNA hsa_circ_0000285 and miR-599 in thyroid cancer. *Eur Rev Med Pharmacol Sci.* 2020;24(13):7219.
22. Vo JN, Cieslik M, Zhang Y, et al. The landscape of circular RNA in cancer. *Cell.* 2019;176(4):869-881.e13.
23. Zhang H-D, Jiang L-H, Sun D-W, et al. CircRNA: a novel type of biomarker for cancer. *Breast Cancer.* 2018;25(1):1-7.
24. Seimiya T, Otsuka M, Iwata T, et al. Aberrant expression of a novel circular RNA in pancreatic cancer. *J Hum Genet.* 2021;66(2):181-191.
25. Li R, Jiang J, Shi H, et al. CircRNA: a rising star in gastric cancer. *Cell Mol Life Sci.* 2020;77(9):1661-1680.
26. Wu Q, et al. Deregulation of circular RNAs in cancer from the perspectives of aberrant biogenesis. Transport and removal. *Front Genet.* 2019;10:16.
27. Liu J, et al. Emerging role of circular RNAs in cancer. *Front Oncol.* 2020;10:663.
28. Zhang W, Zhang S. Downregulation of circRNA_0000285 suppresses cervical cancer development by regulating miR197-3p-ELK1 Axis. *Cancer Manag Res.* 2020;12:8663-8674.
29. Chi BJ, Zhao DM, Liu L, et al. Downregulation of hsa_circ_0000285 serves as a prognostic biomarker for bladder cancer and is involved in cisplatin resistance. *Neoplasma.* 2019;66(2):197-202.
30. Yang D, et al. The interaction between circular RNA hsa_circ_0000285 and miR-599 in thyroid cancer. *Eur Rev Med Pharmacol Sci.* 2020;24(9):4882-4889.
31. Thomson DW, Dinger ME. Endogenous microRNA sponges: evidence and controversy. *Nat Rev Genet.* 2016;17(5):272-283.
32. Dong Y, He D, Peng Z, et al. Circular RNAs in cancer: an emerging key player. *J Hematol Oncol.* 2017;10(1):2.
33. Zhong Y, Du Y, Yang X, et al. Circular RNAs function as ceRNAs to regulate and control human cancer progression. *Mol Cancer.* 2018;17(1):79.
34. Liang ZZ, et al. circRNA-miRNA-mRNA regulatory network in human lung cancer: an update. *Cancer Cell Int.* 2020;20:173.
35. Chen Q, Cai J, Jiang C. CDH2 expression is of prognostic significance in glioma and predicts the efficacy of temozolomide therapy in patients with glioblastoma. *Oncol Lett.* 2018;15(5):7415-7422.

36. Zhang D, Yang X-J, Luo Q-D, et al. Down-regulation of circular RNA_000926 attenuates renal cell carcinoma progression through miRNA-411-dependent CDH2 inhibition. *Am J Pathol.* 2019;189(12):2469-2486.

37. Yao Y, Chen S, Lu NA, et al. LncRNA JPX overexpressed in oral squamous cell carcinoma drives malignancy via miR-944/CDH2 axis. *Oral Dis.* 2021;27(4):924-933.

38. Gao S, et al. MicroRNA-194 regulates cell viability and apoptosis by targeting CDH2 in prostatic cancer. *Onco Targets Ther.* 2018;11:4837-4844.

39. Wan Y, Zhang X, Leng H, et al. Identifying hub genes of papillary thyroid carcinoma in the TCGA and GEO database using bioinformatics analysis. *PeerJ.* 2020;8:e9120.

40. Zhang W, Zhu L, Yang G, et al. Hsa_circ_0026134 expression promoted TRIM25- and IGF2BP3-mediated hepatocellular carcinoma cell proliferation and invasion via sponging miR-127-5p. *Biosci Rep.* 2020;40(7):BSR20191418.

41. Liang M, Yao W, Shi B, et al. Circular RNA hsa_circ_0110389 promotes gastric cancer progression through upregulating SORT1 via sponging miR-127-5p and miR-136-5p. *Cell Death Dis.* 2021;12(7):639.

42. Chang S, Sun L, Feng G. SP1-mediated long noncoding RNA POU3F3 accelerates the cervical cancer through miR-127-5p/FOXD1. *Biomed Pharmacother.* 2019;117:109133.

SUPPORTING INFORMATION

Additional supporting information may be found in the online version of the article at the publisher's website.